

A THREE-DIMENTIONAL SIMULATION OF THE TIDALLY MODULATED PLUME IN THE RIVER ENTRANCE REGION

Nguyen Minh Huan

*Department of Hydro-Meteorology and Oceanography
College of Science, VNU*

Abstract. A three dimensional mathematical model is presented to compute the water level, velocity and salinity distributions in stratified coastal waters and tidally modulated plume of the river entrance region. The model system consists of hydrodynamic, transport and turbulence closure models. In the hydrodynamic model component, the Navier-Stokes equations are solved with the hydrostatic assumption and the Boussinesq approximation. The transport model consists of the water temperature and salinity transport models. The variations in the water temperature and salinity influence the water density, and in return the velocity field. The equations of momentum and continuity are solved numerically using the mode-splitting technique. As the turbulence model, a one-equation k -epsilon turbulence model is applied. In the transport model the three-dimensional advective diffusion equation are solved. The model is applied to a rectangle basin enclosed by a coastal boundary and three open sea boundaries, tidal forcing is imposed in the form of a frictionless Kelvin wave with O_1 frequency entering at the western boundary, freshwater loading was taken into account at location of one river mouth, which reached a total of $1000\text{m}^3\text{s}^{-1}$.

1. Introduction

An estuary is an area of interaction between salt and fresh water. The most common definition used that states "an estuary is a semi-enclosed coastal body of water which has a free connection with the open sea and within which sea water is measurably diluted with fresh water derived from land drainage". The estuarine influence may extend to nearshore coastal waters where seawater is diluted by land drainage but beyond the confines of emergent land-masses.

The classic definition of an estuary includes these three characteristics: semienclosed, free connection with the open sea, and fresh water derived from land drainage. These three characteristics govern the concentration of seawater; therefore, salinity is the key to estuarine classification. The mixing of fresh water and seawater produces density gradients that drive distinctive estuarine (gravitational) circulation patterns.

These circulation and shoaling patterns differ with each estuary system according to the depth, tidal amplitude and phase at the mouth, and the amount of fresh water flowing into the basin.

The tide that approaches the mouth of the estuary is the result of all the astronomical, meteorological, seismic, and man-made factors affecting amplitude and frequency of the wave. As the tide enters the estuary, it is greatly influenced by the river depth, width, and discharge.

Superimposed on this tidal action is the freshwater/saltwater interaction. Salt water will advance up a system until the tidal flow can no longer overcome the riverflow. Depending on the relationship between tidal flow and river flow, the estuary can be classified by its salinity structure and resulting circulation patterns.

2. Theoretical considerations

To simulate wind driven circulation and density currents that occur in coastal waters especially in estuary stratified by salinity and temperature layers causing significant lateral density gradients, three-dimensional mathematical model are necessary. The developed three-dimensional mathematical model is capable of computing the water level and water particle velocity distribution in three principal directions by solving the Navier-Stokes equations using the Boussinesq approximation and the assumption of vertical hydrostatic equilibrium, the continuity equation and equations of temperature and salinity.

2.1 Governing equations of the model

The basic equations in the three-dimensional cartesian coordinate system are:

$$\frac{\partial u}{\partial t} + u \frac{\partial u}{\partial x} + v \frac{\partial u}{\partial y} + w \frac{\partial u}{\partial z} - fv = -\frac{1}{\rho_0} \frac{\partial p}{\partial x} + \frac{\partial}{\partial z} \left(\nu_T \frac{\partial u}{\partial z} \right) + \frac{\partial}{\partial x} \tau_{xx} + \frac{\partial}{\partial y} \tau_{yx} \quad (2.1)$$

$$\frac{\partial v}{\partial t} + u \frac{\partial v}{\partial x} + v \frac{\partial v}{\partial y} + w \frac{\partial v}{\partial z} + fu = -\frac{1}{\rho_0} \frac{\partial p}{\partial y} + \frac{\partial}{\partial z} \left(\nu_T \frac{\partial v}{\partial z} \right) + \frac{\partial}{\partial x} \tau_{xy} + \frac{\partial}{\partial y} \tau_{yy} \quad (2.2)$$

$$\frac{\partial I}{\partial z} = -\rho g \quad (2.3)$$

$$\frac{\partial u}{\partial x} + \frac{\partial v}{\partial y} + \frac{\partial w}{\partial z} = 0 \quad (2.4)$$

$$\frac{\partial T}{\partial t} + u \frac{\partial T}{\partial x} + v \frac{\partial T}{\partial y} + w \frac{\partial T}{\partial z} = \frac{1}{\rho_0 c_p} \frac{\partial I}{\partial z} + \frac{\partial}{\partial z} \left(\lambda_T \frac{\partial T}{\partial z} \right) + \frac{\partial}{\partial x} \left(\lambda_H \frac{\partial T}{\partial x} \right) + \frac{\partial}{\partial y} \left(\lambda_H \frac{\partial T}{\partial y} \right) \quad (2.5)$$

$$\frac{\partial S}{\partial t} + u \frac{\partial S}{\partial x} + v \frac{\partial S}{\partial y} + w \frac{\partial S}{\partial z} = \frac{\partial}{\partial z} \left(\lambda_T \frac{\partial S}{\partial z} \right) + \frac{\partial}{\partial x} \left(\lambda_H \frac{\partial S}{\partial x} \right) + \frac{\partial}{\partial y} \left(\lambda_H \frac{\partial S}{\partial y} \right), \quad (2.6)$$

where (u, v, w) are the components of the current, T denotes the temperature, S the salinity, $f = 2\Omega \sin\phi$ the Coriolis frequency, $\Omega = 2\pi/86164$ rad/s the rotation

frequency of the Earth, g the acceleration of gravity, p the pressure, ν_T and λ_T the vertical eddy viscosity and diffusion coefficients, λ_H the horizontal diffusion coefficient for salinity and temperature, ρ the density, ρ_0 a reference density, c_p the specific heat of seawater at constant pressure and $I(x, y, z, t)$ solar irradiance.

The horizontal components of the stress tensor are defined by

$$\tau_{xx} = 2\nu_H \frac{\partial u}{\partial x} \quad (2.7)$$

$$\tau_{yx} = \tau_{xy} = \nu_H \left(\frac{\partial u}{\partial y} + \frac{\partial v}{\partial x} \right) \quad (2.8)$$

$$\tau_{yy} = 2\nu_H \frac{\partial v}{\partial y}, \quad (2.9)$$

where ν_H is the horizontal diffusion coefficient for momentum.

The numerical solutions of the model equations are greatly simplified by introducing a new vertical coordinate that transforms both the surface and the bottom into coordinate of surfaces (Phillips 1957).

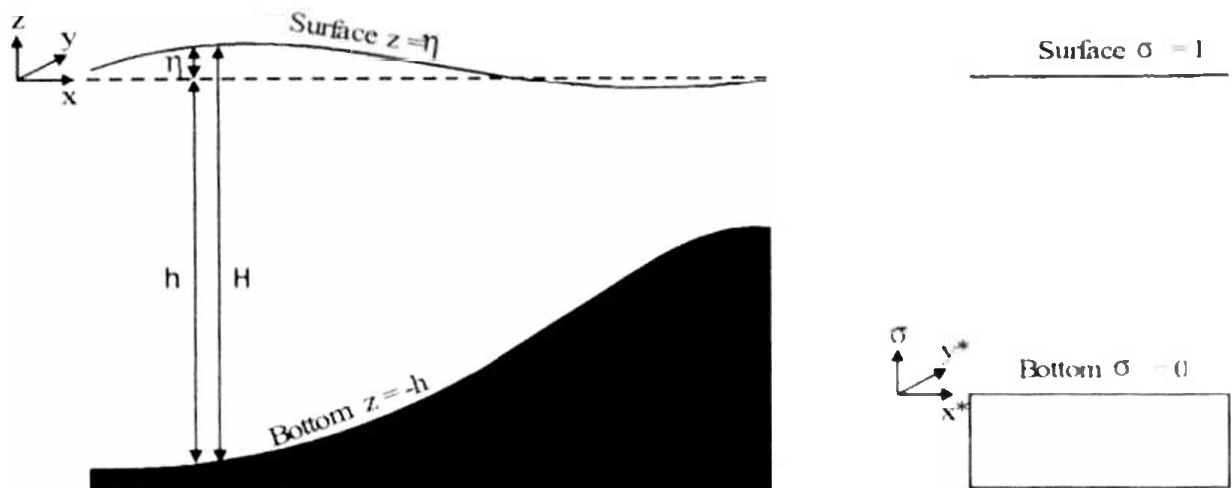


Figure 1.1. The σ -coordinate transformation in the vertical

The following coordinate transformation is applied:

$$(t^*, x^*, y^*, z^*) = (t, x, y, Lf(\sigma)), \quad (2.10)$$

where

$$\sigma = \frac{z + h}{\zeta + h} = \frac{z + h}{H} \quad (2.11)$$

is the commonly used σ -coordinate varying between 0 at the bottom and 1 at the surface. Taking $f(0) = 0$ and $f(1) = 1$ the equation of the bottom takes the simple

form $z^* = 0$ while the moving surface transforms into $z^* = L$. This is further illustrated in Figure 1.1.

The transformed versions of the equations of horizontal momentum, hydrostatic equilibrium, temperature, salinity and continuity are given by

$$\begin{aligned} & \frac{1}{J} \frac{\partial}{\partial t^*} (Ju) + \frac{1}{J} \frac{\partial}{\partial x^*} (Ju^2) + \frac{1}{J} \frac{\partial}{\partial y^*} (Jvu) + \frac{1}{J} \frac{\partial}{\partial z^*} (Jw^*u) - fv \\ &= -g \frac{\partial \zeta}{\partial x^*} - \frac{1}{\rho_0} \frac{\partial P_a}{\partial x^*} + Q_1 + \frac{1}{J} \frac{\partial}{\partial z^*} \left(\frac{v_T}{J} \frac{\partial u}{\partial z^*} \right) \\ & \quad + \frac{1}{J} \frac{\partial}{\partial x^*} (J\tau_{xx}) + \frac{1}{J} \frac{\partial}{\partial y^*} (J\tau_{yx}), \end{aligned} \quad (2.12)$$

$$\begin{aligned} & \frac{1}{J} \frac{\partial}{\partial t^*} (Jv) + \frac{1}{J} \frac{\partial}{\partial x^*} (Juv) + \frac{1}{J} \frac{\partial}{\partial y^*} (Jv^2) + \frac{1}{J} \frac{\partial}{\partial z^*} (Jw^*v) + fu \\ &= -g \frac{\partial \zeta}{\partial y^*} - \frac{1}{\rho_0} \frac{\partial P_a}{\partial y^*} + Q_2 + \frac{1}{J} \frac{\partial}{\partial z^*} \left(\frac{v_T}{J} \frac{\partial v}{\partial z^*} \right) \\ & \quad + \frac{1}{J} \frac{\partial}{\partial x^*} (J\tau_{xy}) + \frac{1}{J} \frac{\partial}{\partial y^*} (J\tau_{yy}), \end{aligned} \quad (2.13)$$

$$\frac{1}{J} \frac{\partial q_d}{\partial z^*} = b; \quad (2.14)$$

$$\begin{aligned} & \frac{1}{J} \frac{\partial}{\partial t^*} (JT) + \frac{1}{J} \frac{\partial}{\partial x^*} (JuT) + \frac{1}{J} \frac{\partial}{\partial y^*} (JvT) + \frac{1}{J} \frac{\partial}{\partial z^*} (Jw^*T) \\ &= \frac{1}{J\rho_0 c_p} \frac{\partial T}{\partial z^*} + \frac{1}{J} \frac{\partial}{\partial z^*} \left(J\lambda_\tau \frac{\partial T}{\partial z^*} \right) \\ & \quad + \frac{1}{J} \frac{\partial}{\partial x^*} \left(J\lambda_H \frac{\partial T}{\partial x^*} \right) + \frac{1}{J} \frac{\partial}{\partial y^*} \left(J\lambda_H \frac{\partial T}{\partial y^*} \right), \end{aligned} \quad (2.15)$$

$$\begin{aligned} & \frac{1}{J} \frac{\partial}{\partial t^*} (JS) + \frac{1}{J} \frac{\partial}{\partial x^*} (JuS) + \frac{1}{J} \frac{\partial}{\partial y^*} (JvS) + \frac{1}{J} \frac{\partial}{\partial z^*} (Jw^*S) \\ &= \frac{1}{J} \frac{\partial}{\partial z^*} \left(J\lambda_\tau \frac{\partial S}{\partial z^*} \right) + \frac{1}{J} \frac{\partial}{\partial x^*} \left(J\lambda_H \frac{\partial S}{\partial x^*} \right) \\ & \quad + \frac{1}{J} \frac{\partial}{\partial y^*} \left(J\lambda_H \frac{\partial S}{\partial y^*} \right), \end{aligned} \quad (2.16)$$

$$\frac{1}{J} \frac{\partial}{\partial t^*} (Jv) + \frac{1}{J} \frac{\partial}{\partial x^*} (Ju) + \frac{1}{J} \frac{\partial}{\partial y^*} (Jv) + \frac{1}{J} \frac{\partial}{\partial z^*} (Jw^*) = 0. \quad (2.17)$$

2.2. Turbulence schemes

One of the most intricate problems in oceanographic modelling is an adequate parameterisation of vertical exchange processes. In the present model they are represented through the eddy coefficients ν_T and λ_T . Values for these two parameters are to be provided by a turbulence scheme.

A large variety of turbulence parameterisations with a substantial range of complexity have been proposed and validated in the literature. The selection of a suitable scheme is often a difficult task since it depends on the type of physical processes specific for the simulated area (e.g. tides, thermoclines, river fronts,...).

In analogy with molecular diffusion where the eddy viscosity and diffusion coefficients are proportional to the mean velocity times and the mean free path of the molecules, the eddy coefficients ν_T and λ_T are considered as the product of a turbulent velocity scale and a length scale l usually denoted by the Kolmogorov-Prandtl "mixing length". A commonly used velocity scale is the square root \sqrt{k} of the turbulent kinetic energy. This parameter can be obtained by solving a transport equation. The most general form of this equations, as used in the program, is written as

$$(T + A_h + A_v - D_h)k - \frac{1}{J} \frac{\partial}{\partial z^*} \left(\left(\frac{\nu_T}{\sigma_k} + \nu_b \right) \frac{1}{J} \frac{\partial k}{\partial z^*} \right) = \nu_T M^2 - \lambda_T N^2 - \varepsilon, \quad (2.18)$$

where the time derivative, the horizontal and vertical advection as the diffusion operators are defined by

$$T(k) = \frac{1}{J} \frac{\partial}{\partial t} (Jk) \quad (2.18a)$$

$$A_h(k) = \frac{1}{J} \frac{\partial}{\partial x} (Juk) + \frac{1}{J} \frac{\partial}{\partial y} (Jvk) \quad (2.18b)$$

$$A_v(k) = \frac{1}{J} \frac{\partial}{\partial z^*} (Jwk) \quad (2.18c)$$

$$D_h(k) = \frac{1}{J} \frac{\partial}{\partial x} \left(J \lambda_H^k \frac{\partial k}{\partial x} \right) + \frac{1}{J} \frac{\partial}{\partial y} \left(J \lambda_H^k \frac{\partial k}{\partial y} \right), \quad (2.18d)$$

N^2 and M^2 are squared buoyancy and shear frequencies given by

$$N^2 = \frac{g}{J} \left(\beta_T \frac{\partial T}{\partial z^*} - \beta_S \frac{\partial S}{\partial z^*} \right) \quad (2.19)$$

$$M^2 = \frac{1}{J^2} \left(\left(\frac{\partial u}{\partial z^*} \right)^2 + \left(\frac{\partial v}{\partial z^*} \right)^2 \right) \quad (2.20)$$

and ϵ denotes the dissipation rate of turbulence energy. The dissipation rate is parameterised according to

$$\epsilon = \epsilon_0 \frac{k^{3/2}}{l} \quad (2.21)$$

where ϵ_0 is a constant determined by $\epsilon_0 = 0.188$.

All turbulence transport equations are solved with the same horizontal diffusion coefficient λ_H which is the same as the one used in the equations of temperature and salinity.

The eddy coefficients are then expressed as

$$v_T = S_u k^2 / \epsilon + v_b, \quad \lambda_T = S_b k^2 / \epsilon + \lambda_b, \quad (2.22)$$

where v_b, λ_b are prescribed background coefficients, $v_b = 10^{-4} [m^2/s]$; $\lambda_b = 10^{-5} [m^2/s]$ and S_u, S_b are usually referred as the stability functions. Their explicit forms are

$$S_u = \frac{0.108 + 0.0229\alpha_N}{1 + 0.471\alpha_N + 0.0275\alpha_N^2} \quad (2.23)$$

$$S_b = \frac{0.177}{1 + 0.403\alpha_N},$$

where $\alpha_N = \frac{k^2}{\epsilon^2} N^2$ (2.24)

One-equation k-epsilon turbulence model is used for parameterisation for the mixing length and dissipation rate. When one-equation model is chosen, the k-equation is still solved with ϵ modelled according to (2.21) while l is determined using the formulation, initially proposed by Blackadar (1962), has the form

$$\frac{1}{l} = \frac{1}{l_1} + \frac{1}{l_2} + \frac{1}{l_u}. \quad (2.25)$$

Horizontal diffusion terms are meant to parameterize subgrid scale processes, in practice the horizontal diffusivity v_H and λ_H are usually required to damp small scale computational noise they are taken proportional to the horizontal grid spacings and the magnitude of the velocity deformation tensor in analogy with Smagorinsky's (1963) parameterisation

$$v_H = C_{m0} \Delta x \Delta y D_T \quad \text{and} \quad \lambda_H = C_{s0} \Delta x \Delta y D_T. \quad (2.26)$$

2.3 Boundary and initial conditions

Coastal boundaries are considered as impregnable walls. This means that all currents, advective and diffusive fluxes are set to zero

$$\bar{U} = 0, \quad u = 0, \quad Ju\psi = 0, \quad \lambda_H \frac{\partial \psi}{\partial x} = 0 \quad (2.277)$$

$$\bar{V} = 0, \quad v = 0, \quad Jv\psi = 0, \quad \lambda_H \frac{\partial \psi}{\partial y} = 0. \quad (2.283)$$

Open sea (or river) boundary condition for the 2-D mode need to be supplied for \bar{U} at western and eastern boundaries and for \bar{V} at southern and northern boundaries. A selection can be made between different types of open boundary conditions. They have the form of a radiation condition derived using the method of characteristics [Hedstrom 1979], [Roed and Cooper, 1987], [Ruddick, 1995], [Randall J. LeVeque 1997]. This is based on the integration of the equations for the incoming and outgoing Riemann variables

$$(R_+^u, R_+^v) = (\bar{U} \pm c\zeta, \bar{V} \pm c\zeta) \quad (2.29)$$

3. Numerical simulation

The aim of the test is to simulate the evolution of a tidally modulated river plume using the following conditions of a basin with water depth ranging from 3m in the shoreline to 20m in the offshore boundary. The computational domain, has the form of a rectangle basin enclosed by a coastal (solid) boundary and three open sea boundaries. For convenience, the coastal boundary will be denoted by the southern boundary, the latter by the western, eastern cross-shore boundaries and the northern alongshore boundary. The basin has a length of 120 km, a width of 40 km, in the southern boundary there is the river mouth situated in the distance of 60 km from the western boundary and discharge water to basin inside one harbor constructed by 2 groins. The horizontal resolution of grid is 500m and 20 levels are used in the vertical. The area is filled initially with seawater having a uniform salinity of 30 PSU.

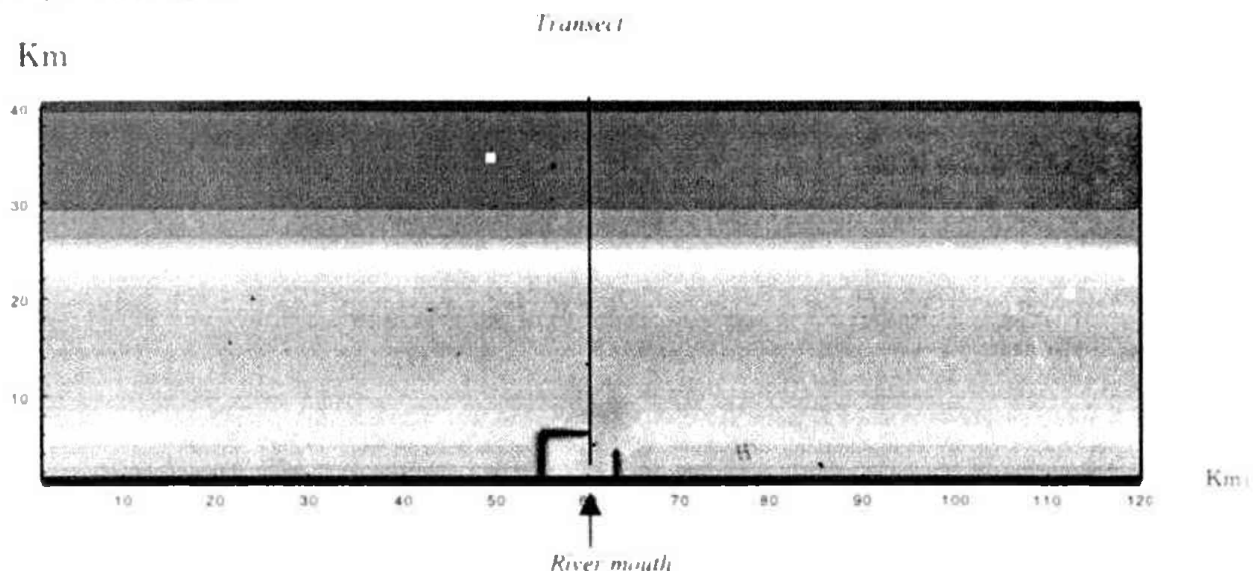


Figure 3.1: The computational domain

Tidal forcing is imposed in the form of a frictionless Kelvin wave with frequency of O_1 entering at the western boundary and propagating along the coast [Van Rijn, 1989 and Ruddick et. al., 1995]. The incoming Riemann variable, specialized at the western boundary, then takes the form

$$R_+ = \bar{U} + c\zeta = 2 cF_{\text{bar}} = 2cAe^{f y/c} \cos\omega t, \quad (3.1)$$

where the Coriolis frequency is evaluated at a latitude of 20° , ω is the O_1 tidal frequency, $A = 0.8\text{m}$ and \bar{U} , c , ζ are the depth-integrated alongshore current, the barotropic wave speed and the surface elevation. The amplitude of the wave decreases exponentially with distance to the coast with a decay scale given by the barotropic Rossby radius $c/f \sim 120$ km. The amplitude $Ae^{f y/c}$ of the harmonic function F_{bar} is stored for each open boundary node.

A zero normal gradient condition is selected at the eastern and northern boundaries, i.e.

$$\begin{aligned} \frac{\partial}{\partial x}(\bar{U} - c\zeta) &= 0 \\ \frac{\partial}{\partial y}(\bar{V} - c\zeta) &= 0. \end{aligned} \quad (3.2)$$

The later condition is justified by the fact that the width of the basin is much smaller than the external Rossby radius c/f .

Since the value of ζ is unknown at the river mouth, the open boundary condition at the inlet is no longer defined in terms of the incoming Riemann variable but by specifying the cross-shore component of the depth integrated current. This is given as the sum of a residual value, representing the river discharge, and a tidal component

$$V = cF_{\text{bar}} = \frac{Q_d}{W} + A_r H \cos(\omega t - \varphi_r) \quad (3.3)$$

where $Q_d = 1000 \text{ m}^3/\text{s}$ is the river discharge, $W = 500\text{m}$ the width of the inlet and $A_r = 0.6 \text{ m/s}$ the amplitude of the tidal current at the mouth of the river. The phase φ_r is determined by

$$\varphi_r = \omega \frac{D_r}{c} - \frac{\pi}{2}, \quad (3.4)$$

where $D_r = 26.0 \text{ km}$ so that D_r/c represents the time travelled by the Kelvin wave from the western boundary to the river mouth. Observations in the river plume show that the alongshore and cross-shore component are anti-phase, which explains the use of the factor $\pi/2$ [Van Rijn, 1989].

In addition to the previous conditions for the 2-D mode, open boundary conditions have to be imposed during the final run for the horizontal velocity deviations (u' , v') and the salinity S .

At the open sea boundaries a zero normal gradient condition is taken for all quantities. In the case of salinity this procedure is a reasonable approximation since the plume never intersects the western and northern boundary while the cross-boundary gradient is much smaller than the along-boundary gradient at the eastern boundary.

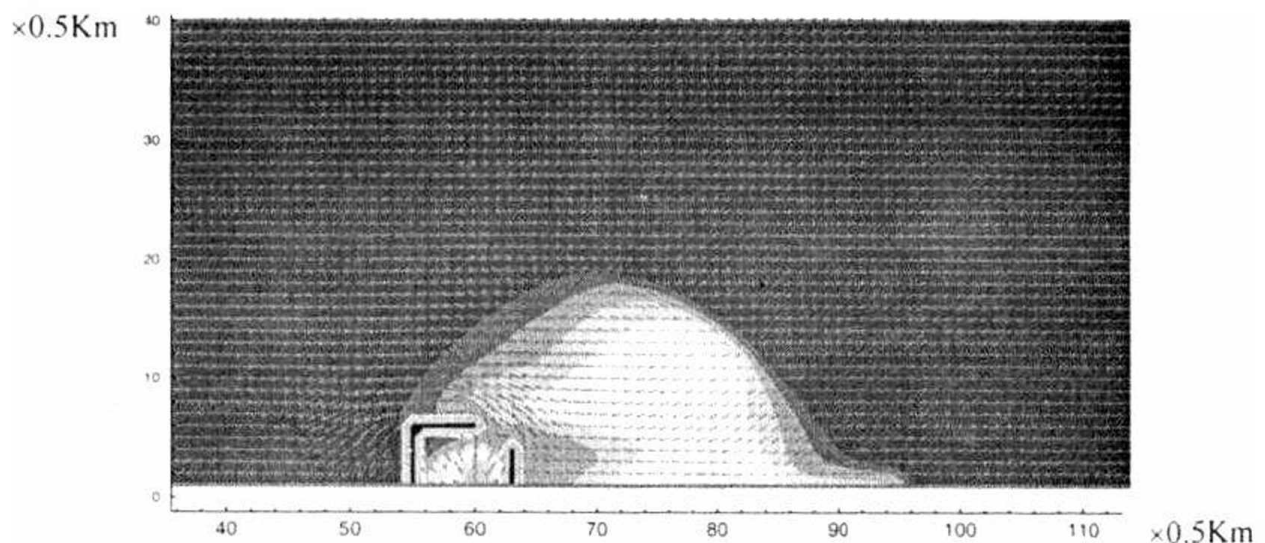
The default conditions are no longer applicable at the river mouth where v' and S are specified in the form of a two-layer stratification

$$\begin{aligned} S &= 10 \text{ PSU}, & v' &= 0.6 \text{ [m.s}^{-1}\text{]} & \text{if } z > -\delta \\ v' &= -0.2 \text{ [m.s}^{-1}\text{]} & & & \text{if } -H \leq z \leq -\delta, \end{aligned} \quad (3.5)$$

where $\delta = 5 \text{ m}$ is the specified depth of the plume layer at the mouth. In this way fresh water is released through the surface layer whereas saltier seawater flows into the estuary through the bottom layer. A zero gradient condition is applied for salinity in the bottom layer.

4. Discussion

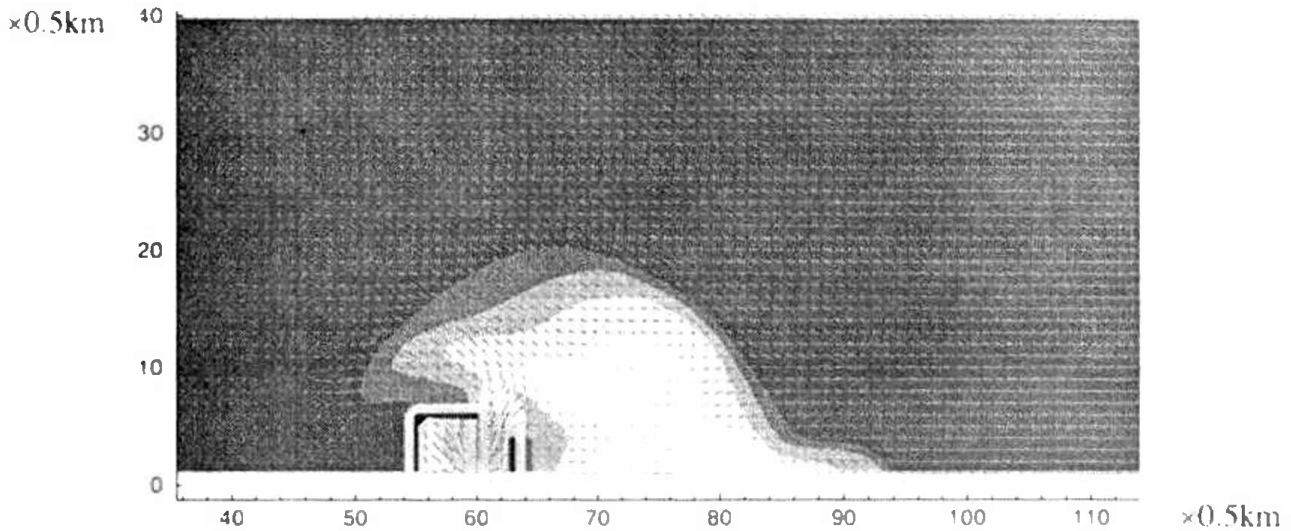
Although the developed program is able to examine the role of different physical forcing mechanism (bathymetry, tides, wind, wave) on the plume structure, the intention here is to test some of the above-mentioned forcing and the role of the Smagorinsky formulation for horizontal diffusion and the upwind scheme for the advection of momentum.



Figures 4.1. Surface distribution of current and salinity after 50h simulation (final run)

Figures 4.1 – 4.5 clearly show how the plume evolves during a tidal cycle. At the time when the alongshore current reverses sign and the outflow reaches its

maximum, a new blob of fresh water enters the basin, moving seawards (Figure 4.1)



Figures 4.2. Surface distribution of current and salinity after 52h simulation

As the eastward directed tidal wave becomes stronger, the fresh water patch is deflected to the right (Figure 4.3).

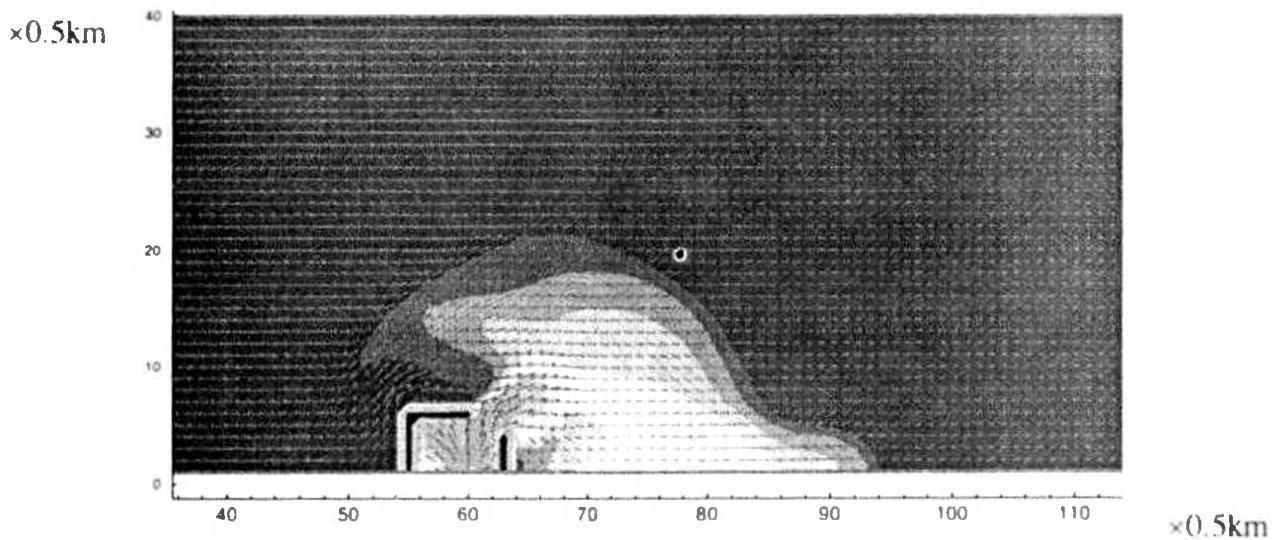


Figure 4.3: Surface distribution of current and salinity after 54h simulation

During this phase of the tide both the bulge and the coastal plume expand seawards. When the tidal current reverses sign again and turns to the west, the current inside the plume is first southeastwards pushing the bulge towards the coast (Figure 4.4).

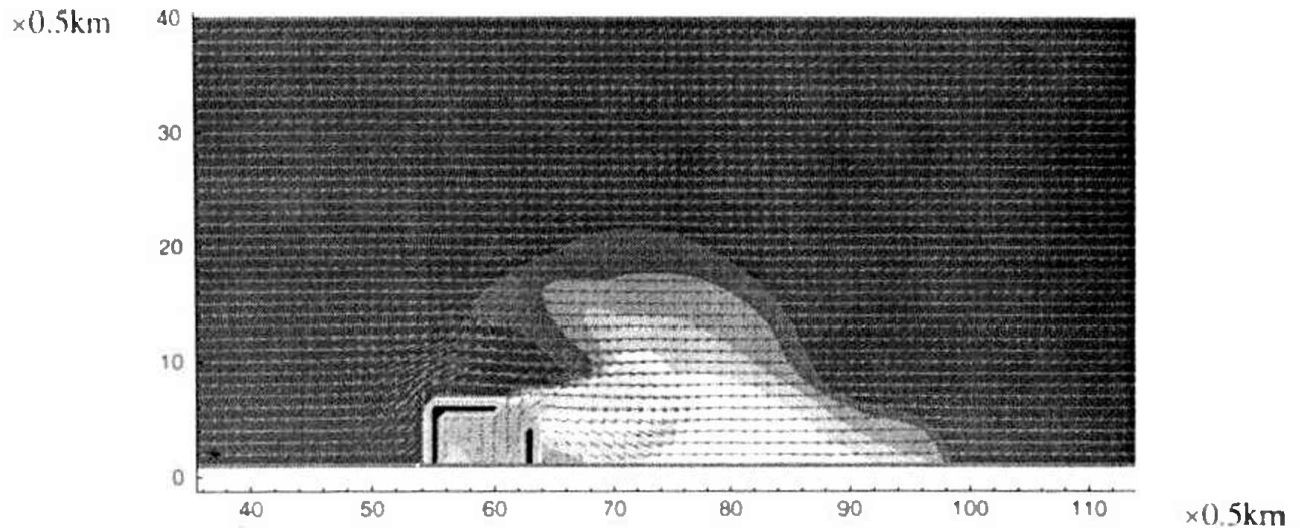


Figure 4.4: Surface distribution of current and salinity after 56h simulation

And finally southwestwards reducing the extent of the bulge and the coastal plume (Figure 4.5). The main feature here is that the bulge and the coastal plume oscillate with the tide.

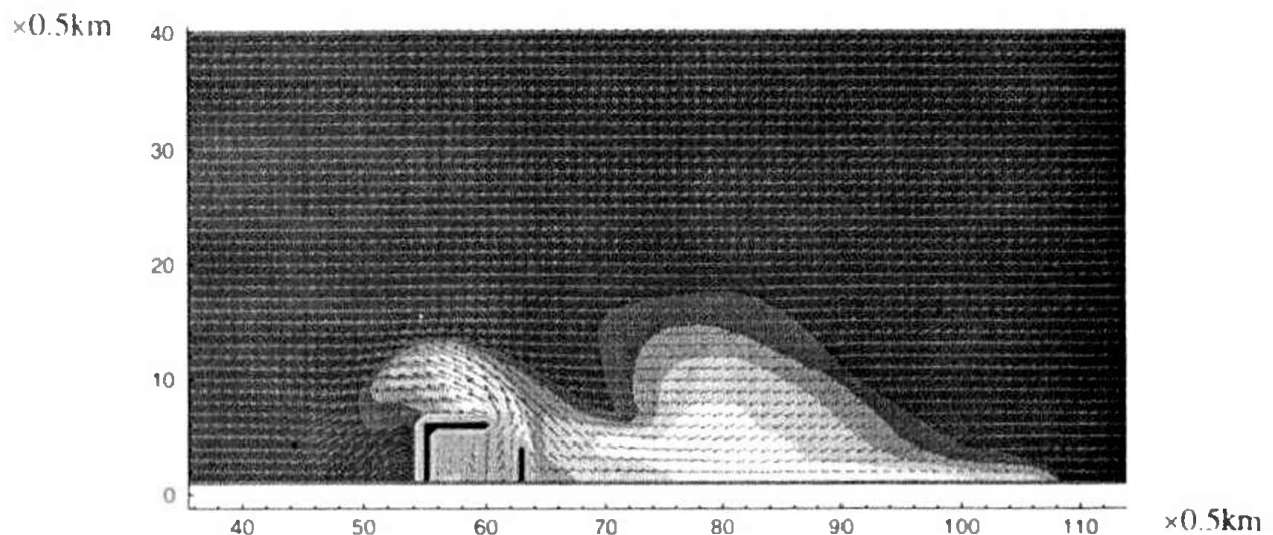


Figure 4.5: Surface distribution of current and salinity after 62h simulation

The current and salinity fields along the transects show the presence of an estuarine-type circulation (Figure 4.5). In the cross-shore transect upwelling takes place at the coast while downwelling occurs at the edge of the plume by the convergence of the surface outflow current. A similar phenomenon is seen in the coastal jet where downwelling motions are created by the convergence of the coastal jet. In the case of a non-tidal plume the plume layer is shallower and the frontal gradients are stronger compared to the tidal case where turbulent diffusion increases the depth of the surface layer and reduces the vertical stratification.

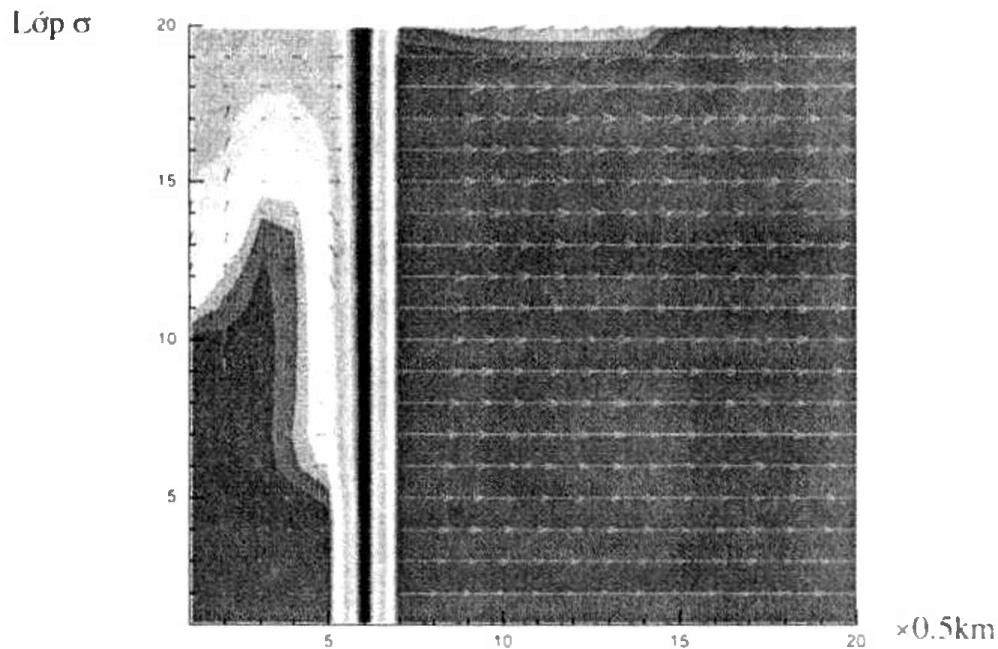


Figure 4.6: Cross-sectional distribution of current and salinity after 66h simulation in the σ -coordinate

5. Concluding remarks

This paper presented a three dimensional model which consists of a circulation model, a transport model, and a one equation k-epsilon turbulence model. The use of three-dimensional models is unavoidable in all cases where the influence of density distribution cannot be neglected or and in wind driven flows, which have typically three-dimensional character. The developed model also must to be well calibrated and verified with another numerical experimental and prototype data.

Questions about this article and source code in FORTRAN of program can be addressed to Nguyen Minh Huan, Faculty of Hydro-Meteorology and Oceanography, College of Natural Sciences.

Acknowledgments. This work has been supported by the Hanoi University of Science project coded KT – 2000-23 and Natural Science Council of Vietnam (2001-2003) project coded 7317001.

REFERENCES

1. Blackadar A.K., The vertical distribution of wind and turbulent exchange in a neutral atmosphere, *Journal of Geophysical Research*, **67**(1962), 3095–3102.
2. Blumberg A.F. and Mellor G.L., A description of a three-dimensional coastal ocean circulation model. In: N.S.Heaps (Editor), *Three-dimensional Coastal Ocean Models, Coastal and Estuarine Sciences*, Vol.4, American Geophysical Union, Washington D.C., 1987pp.1 –16.

3. Davies A.M., A bottom boundary layer-resolving three-dimensional tidal model: A sensitivity study of eddy viscosity formulation, *Journal of Physical Oceanography*, **23**(1993) 1437 –1453.
4. Phillips N.A., A coordinate system having some special advantages for numerical forecasting, *Journal of Meteorology*, **14**(1957), 184–185.
5. Hedstrom G.W., Nonreflecting boundary conditions for nonlinear hyperbolic systems, *Journal of Computational Physics*, **30**(1979) 222 –237.
6. Leo C. van Rijn, Principles of fluid flow and surface in rivers, estuaries, seas and oceans, *Aqua Publications*, 1989, pp. 216-226.
7. Roed L.P. and Cooper C.K., *A study of various open boundary conditions for wind-forced barotropic numerical ocean models*, In: J.C.J.Nihoul and B.M.Jamart (Editors), *Three-dimensional models of marine and estuarine dynamics*, Elsevier, Amsterdam, 1987, pp.305 –335.
8. Randall J. LeVeque, *Nonlinear Conservation Laws and Finite Volume Methods for Astrophysical Fluid Flow*, Springer-Verlag, Washington D.C, 1998.
9. Ruddick K.G., *Modelling of coastal processes influenced by the freshwater discharge of the Rhine*, Univ. de Liège, Belgium, 1995, 247 pp.

TAP CHÍ KHOA HỌC ĐHQGHN, KHTN & CN, T. XIX, N₀1, 2003

KẾT QUẢ MÔ PHỎNG 3 CHIỀU CHẾ ĐỘ DÒNG CHẢY VÙNG CỬA SÔNG CHỊU TÁC ĐỘNG CỦA THỦY TRIỀU

Nguyễn Minh Huân

*Khoa Khí tượng Thủy văn và Hải dương học,
Đại học Khoa học Tự nhiên, ĐHQG Hà Nội*

Mô hình thủy động lực 3 chiều được sử dụng trong tính toán mô phỏng mực nước, vận tốc dòng chảy và phân bố độ muối ở vùng nước cửa sông phân tầng chịu tác động của thủy triều. Mô hình bao gồm các phương trình thủy động lực, truyền tải và được khép kín bằng các sơ đồ rôi. Hệ phương trình thủy động lực của mô hình là hệ phương trình Navier-Stokes sử dụng giả thuyết thủy tĩnh và xấp xỉ Boussinesq. Sự biến động của nhiệt độ và độ muối sẽ ảnh hưởng lên mật độ của nước và mật độ biến đổi sẽ ảnh hưởng ngược lại lên trường dòng chảy. Hệ phương trình động lượng và liên tục được giải bằng phương pháp phân tách thành phần, áp dụng mô hình rôi k-epsilon một phương trình. Trong mô hình tải, các phương trình khuếch tán đối lưu ba chiều được sử dụng. Mô hình được áp dụng cho khu vực biển ven bờ có cửa sông với một biên cứng và 3 biên lỏng, mực nước biến động ở biên lỏng phía tây do tác động của sóng triều O_1 , lưu lượng nước sông chảy vào vùng tính có mô phỏng khu vực cảng với giá trị là $1000\text{m}^3.\text{s}^{-1}$. Kết quả tính toán đã mô phỏng được chế độ đặc trưng của dòng chảy 3 chiều vùng cửa sông chịu tác động của thủy triều.